View metadata, citation and similar papers at core.ac.uk
brought to you by CORE
provided by Elsevier - Publisher Connector

Cell, Vol. 119, 285–298, October 15, 2004, Copyright ©2004 by Cell Press

IKKβ/NF-κB Activation Causes Severe Muscle Wasting in Mice

Dongsheng Cai,[1,6] J. Daniel Frantz,[1,6,10]
Nicholas E. Tawa, Jr.,[2,7] Peter A. Melendez,[1,6,11]
Byung-Chul Oh,[1,6] Hart G.W. Lidov,[3,8]
Per-Olof Hasselgren,[2,7] Walter R. Frontera,[4,9]
Jongsoon Lee,[1,6] David J. Glass,[5]
and Steven E. Shoelson[1,6,*]
[1]Research Division
Joslin Diabetes Center
One Joslin Place
[2]Department of Surgery
Beth Israel Deaconess Medical Center
330 Brookline Avenue
Boston, Massachusetts 02215
[3]Division of Genetics
Children's Hospital
300 Longwood Avenue
Boston, Massachusetts 02115
[4]Department of Physical Medicine
and Rehabilitation
Spaulding Rehabilitation Hospital
125 Nashua Street
Boston, Massachusetts 02114
[5]Muscle Program
Regeneron Pharmaceuticals
777 Old Saw Mill River Road
Tarrytown, New York 10591
[6]Department of Medicine
[7]Department of Surgery
[8]Department of Pediatrics
[9]Department of Physical Medicine
and Rehabilitation
Harvard Medical School
Boston, Massachusetts 02115

Summary

Muscle wasting accompanies aging and pathological conditions ranging from cancer, cachexia, and diabetes to denervation and immobilization. We show that activation of NF-κB, through muscle-specific transgenic expression of activated IκB kinase β (MIKK), causes profound muscle wasting that resembles clinical cachexia. In contrast, no overt phenotype was seen upon muscle-specific inhibition of NF-κB through expression of IκBα superrepressor (MISR). Muscle loss was due to accelerated protein breakdown through ubiquitin-dependent proteolysis. Expression of the E3 ligase MuRF1, a mediator of muscle atrophy, was increased in MIKK mice. Pharmacological or genetic inhibition of the IKKβ/NF-κB/MuRF1 pathway reversed muscle atrophy. Denervation- and tumor-induced muscle loss were substantially reduced and survival rates improved by NF-κB inhibition in MISR mice, consistent with a critical role for NF-κB in the pathology of muscle wasting and establishing it as an important clinical target for the treatment of muscle atrophy.

*Correspondence: steven.shoelson@joslin.harvard.edu
[10]Present address: Vertex Pharmaceuticals, 130 Waverly Street, Cambridge, Massachusetts 02139.
[11]Present address: Hewlett Packard Caribe Ltd., P.O. Box 4048, Aguadilla, Puerto Rico 00603.

Introduction

Muscle wasting is a major feature of the cachexia associated with diverse pathologies such as cancer, bacterial sepsis, AIDS, diabetes, and end-stage heart, kidney, and chronic obstructive pulmonary disease (Tisdale, 1997; Argiles and Lopez-Soriano, 1999). During cachexia, muscle protein breakdown occurs well out of proportion to the catabolic effects of cachexia seen in other tissues, causing generalized weakness and debilitation, which in respiratory muscles may be sufficiently severe to ultimately lead to asphyxia and death. Muscle wasting seen in such catabolic states appears to be mediated predominantly by activation of ubiquitin- and proteasome-dependent pathways (Lecker et al., 1999), perhaps through increases in the expression of relevant proteins, including ubiquitin E2-conjugating enzyme and subunits of the proteasome. Genetic deletion of either of two recently discovered muscle-specific E3 ligases, atrogin-1/MAFbx or MuRF1 (muscle RING finger protein 1), protects against muscle atrophy following denervation and disuse (Bodine et al., 2001; Glass, 2003).

Several cytokines have been implicated in the pathogenesis of muscle wasting, most notably TNF-α, a proinflammatory cytokine that was originally called "cachectin" (Tisdale, 1997; Argiles and Lopez-Soriano, 1999). Concentrations of TNF-α are often elevated in the circulations of patients with sepsis or cancer, contributing to negative nitrogen balance—but, by itself, TNF-α may be insufficient to cause muscle wasting (Moldawer et al., 1987; Fong et al., 1989; Mullen et al., 1990). IL-1β, IL-6, IFN-γ, TGFβ, LIF, and other related cytokines have been implicated as potential mediators of muscle wasting or atrophy, suggesting that clinical syndromes might involve synergistic effects of combinations of cytokines (Argiles and Lopez-Soriano, 1999).

Since NF-κB in muscle is activated by disuse (Hunter et al., 2002) or sepsis (Penner et al., 2001), it might play a role in the pathogenesis of these conditions, although alternative intracellular pathways including caspases and JNK/AP-1 have also been shown to be activated in muscle by cytokines (Coletti et al., 2002; Stewart et al., 2004). Consistent with a role for NF-κB, in vitro blockade inhibits protein loss in C2C12 myotubes (Li and Reid, 2000). Although detailed mechanisms of NF-κB have been established in innate immunity, inflammation, and apoptosis, its in vivo functions in muscle are unknown. In cells of the immune and inflammatory systems, NF-κB is a central integration site for proinflammatory signals and a master regulator of related target genes. Numerous inputs that activate NF-κB in addition to TNF-α and IL-1β include bacterial cell wall and viral products, dsDNA, mitogens, and reactive oxygen species (ROS) (Baeuerle and Baltimore, 1996; Rothwarf and Karin,

2000). NF-κB activation in these cells directly increases the production of a whole host of related proteins, including cytokines and chemokines, immune- and antigen-presenting receptors, stress response and acute phase proteins, and other regulators of apoptosis, growth, and host defense. Recent studies in cultured C2C12 muscle cells suggested that TNF-α inhibits myocyte differentiation through NF-κB activation (Guttridge et al., 2000; Langen et al., 2001; Ladner et al., 2003). We have activated and inhibited NF-κB selectively in the skeletal muscle of transgenic mice to further investigate its in vivo functions in this tissue.

Results

Muscle Atrophy in MIKK Mice

Activation of the IκB kinase (IKK) complex promotes IκBα phosphorylation at S32 and S36, which is required for ubiqitination and subsequent proteasomal degradation of IκBα (Yaron et al., 1998). The degradation of IκBα liberates NF-κB and allows it to translocate into the nucleus (Baeuerle and Baltimore, 1996; Delhase et al., 1999; Rothwarf and Karin, 2000). Activation of IKKβ by phosphorylation of S177 and S181 in its kinase activation loop is mimicked by glutamic acid substitutions (Ling et al., 1998; Delhase et al., 1999; Mercurio et al., 1999), whereas the phosphorylation and degradation of IκBα is blocked by S32A and S36A substitutions (Van Antwerp et al., 1996). We have confirmed these results by showing that NF-κB in cells is activated through IKKβ SS177/181EE expression and inhibited by IκBα SS32/36AA expression (see Supplemental Figure S1A at http://www.cell.com/cgi/content/full/119/2/285/DC1/). We have created transgenic mice, with NF-κB either activated or inhibited selectively in skeletal muscle, using a muscle creatine kinase (MCK) promoter to drive the expression of constitutively active IKKβ SS177/181EE or dominant inhibitory IκBα SS32/36AA, respectively (Supplemental Figure S1B). These mice are referred to as MIKK (muscle-specific expression of IKK) or MISR (muscle-specific expression of IκB superrepressor).

Transgenic expression of IKKβ protein in MIKK mice was elevated about 10- to 13-fold over basal endogenous levels in skeletal muscle, was negligible in heart, and was not detectable in other tissues (Figures 1A and 1B). Transgenic Flag-tagged IKKβ is incorporated into IKK signalosomes, as judged both by the presence of IKKα and IKKγ in anti-Flag immunoprecipitates and by the presence of Flag-tagged IKKβ in IKKγ immunoprecipitates (Figure 1C). The decreased amount of IκBα present in MIKK muscle relative to wild-type (wt) indicated that increased IκB kinase activity was having its reported effect, increased degradation of IκBα (Figure 1C). In vitro quantification indicated that kinase activity in MIKK muscle is increased 10-fold in anti-IKKγ immune complex assays, relative to wt littermates, using recombinant IκBα as substrate (Figure 1D). This translates into a 15- ± 2.5-fold increase in NF-κB activity in MIKK muscle, compared to wt littermates, as judged by both EMSA and ELISA assays (Figure 1E). This degree of NF-κB activation matches that seen in a model of muscle atrophy (Hunter et al., 2002). The EMSA and ELISA assays measure the amount of NF-κB that is free to translocate into the nucleus; unrelated transcription factors, including Oct1, were not activated in MIKK mice (Figure 1E and see Supplemental Figure S1C on the *Cell* web site). MIKK mice exhibit a profound syndrome of muscle wasting. In contrast, MISR mice lack an overt phenotype despite high-level expression of the transgenic IκBα superrepressor (Figure 1F). Basal NF-κB activity is inhibited by 80% in MISR muscle relative to wt (Figure 1E).

We have characterized the muscle wasting phenotype in male MIKK mice, although both sexes were equivalently affected. Two independent transgenic lines have identical phenotypes. MIKK mice are viable and appear normal at birth. As they mature, gross appearance and snout-to-anus length remain normal, although MIKK body weights are reduced due to decreases in skeletal muscle mass (Figures 1G). All other organs and tissues have normal weights and histological appearances. Muscles of both the limbs and trunk were affected, and relative reductions in muscle mass increased with age. Circulating creatine kinase levels were normal. Histological examination revealed smaller muscle fibers than wt littermates, without evidence of central nuclei, inflammatory infiltrates, necrotic degeneration, or fibrosis (Figures 1I and 1J). Intramuscular nerves appeared normal. Instead of increasing with age, as occurs normally, cross-sectional areas of muscle fibers in MIKK mice decreased with age (Figure 1H). Fiber and myonuclei numbers remained normal at earlier ages (Supplemental Figures S1D and S1E), suggesting ongoing atrophy in the absence of reduced myogenesis. Decreases in fiber number seen in older animals (Supplemental Figure S1D), along with replacement of muscle by fat (Figures 1I and 1J), are suggestive of chronic atrophy and severe muscle wasting (Mora, 1989). In mature mice, only soleus was unaffected in terms of both weight (Figure 1G) and histology (data not shown), despite high-level expression of the transgene (Figure 1B). Selective sparing of soleus has been seen in both human and rodent cachexia (Tiao et al., 1997; Fang et al., 1998; Carpenter and Karpati, 2001). Immature muscles in MIKK fetuses and neonates, which contain embryonic and neonatal myosin isoforms, were unaffected as well (data not shown), suggesting that adult fast twitch muscles are predominantly affected.

Ex vivo analyses further quantified size and contractile function in muscles of MIKK mice. Tibialis anterior (TA) muscles from 12-week-old mice had normal numbers of muscle fibers, but fiber diameter and cross-sectional area were 56% and 32% of normal, respectively. In addition to being small, muscles from MIKK mice exhibited functional deficits. Maximal force generated by single MIKK fibers was 23% of controls (Supplemental Figure S1E), which corresponds to a 20% reduction when normalized by transverse area (Supplemental Figure S1F). Contraction (unloaded shortening) velocity was reduced by 21% in TA fibers from MIKK mice (Supplemental Figure S1G).

Reversal of the MIKK Phenotype by Transgenic Suppression of IκBα Degradation

Expression of IκB SS32/36AA (superrepressor) in muscle does not induce an obvious phenotype; MISR mice

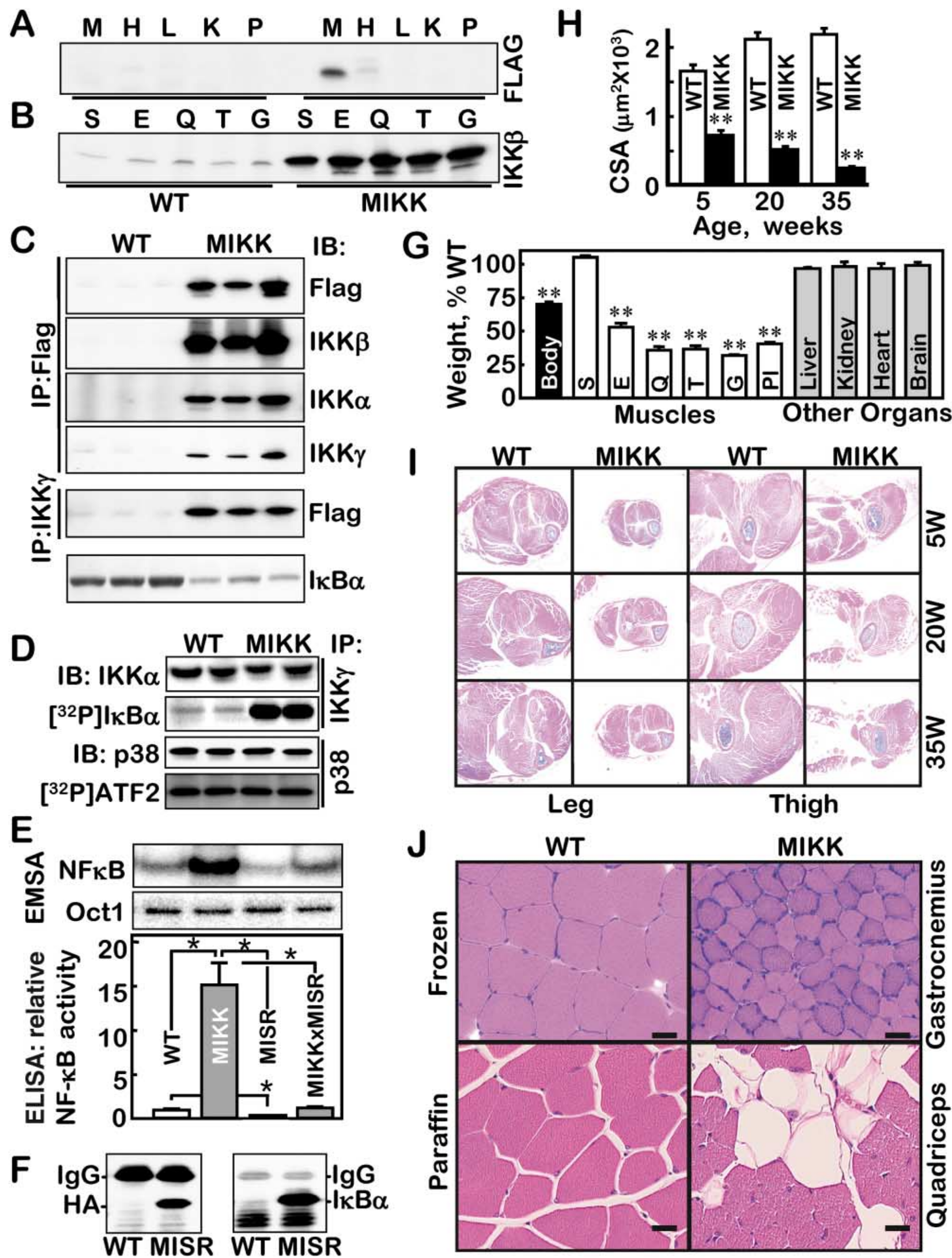

Figure 1. Profound Muscle Atrophy upon Muscle-Specific Activation of IKKβ/NF-κB

Muscle lysates from MIKK mice and wt littermates were separated by SDS-PAGE, and proteins were analyzed by immunoblotting (IB) with (A) anti-Flag antibody that recognizes the transgene but not the endogenous protein and (B) anti-IKKβ antibody that recognizes both proteins. (C) Proteins immunoprecipitated (IP) from lysates of wt or MIKK muscle (n = 3) using anti-Flag or anti-IKKγ antibodies were separated by SDS-PAGE and identified by immunoblotting with anti-Flag, anti-IKKβ, anti-IKKα, or anti-IKKγ antibodies. (Bottom panel) Tissue lysates were separated by SDS-PAGE, and IκBα was identified by immunoblotting with specific antibodies. (D) An immune complex assay used anti-IKKγ antibodies to immunoprecipitate IKK complexes from wt and MIKK muscle lysates. Anti-p38 antibody was used to immunoprecipitate p38 kinase as control. [γ-^{32}P]ATP and either recombinant GST-IκBα or GST-ATF2, respectively, added as substrates, were separated by SDS-PAGE and detected by autoradiography. As loading controls, portions of the immunoprecipitates were separated by SDS-PAGE for Western blotting of IKKα or p38. (E) NF-κB activity was measured in wt, MIKK, MISR, and MIKK x MISR gastrocnemius muscle using both EMSA- (upper) and ELISA-based DNA binding (lower) assays (n = 3). Oct1 activity was measured as control transcriptional factors for all samples. (F) Proteins immunoprecipitated from lysates of wt or MISR muscle using anti-HA antibodies were analyzed by Western blotting using anti-HA and anti-IκBα antibodies. (G) Overall body and individual muscle and organ weights (black, white, or gray bars, respectively) of 12-week-old MIKK mice are expressed as percentages of wt (n = 6). (H) Muscle fiber cross-sectional areas (CSA) were measured in transverse frozen sections of EDL muscles at the indicated ages (wt, open; MIKK, black fill; n = 6–10). (I) Transverse sections taken at the midpoints of MIKK or wt legs and thighs were stained with hematoxylin and eosin (H&E) (12.5× magnification). (K) H&E-stained transverse sections of gastrocnemius (frozen) and quadriceps (fixed) muscles are from 20-week-old mice (200× magnification, scale bar = 35 μm). M, skeletal muscle; H, heart; L, liver; K, kidney; P, pancreas; S, soleus; E, extensor digitorum longus; Q, quadriceps; T, tibialis anterior; G, gastrocnemius; Pl, plantaris ($^{*}p < 0.001$; $^{**}p < 10^{-8}$).

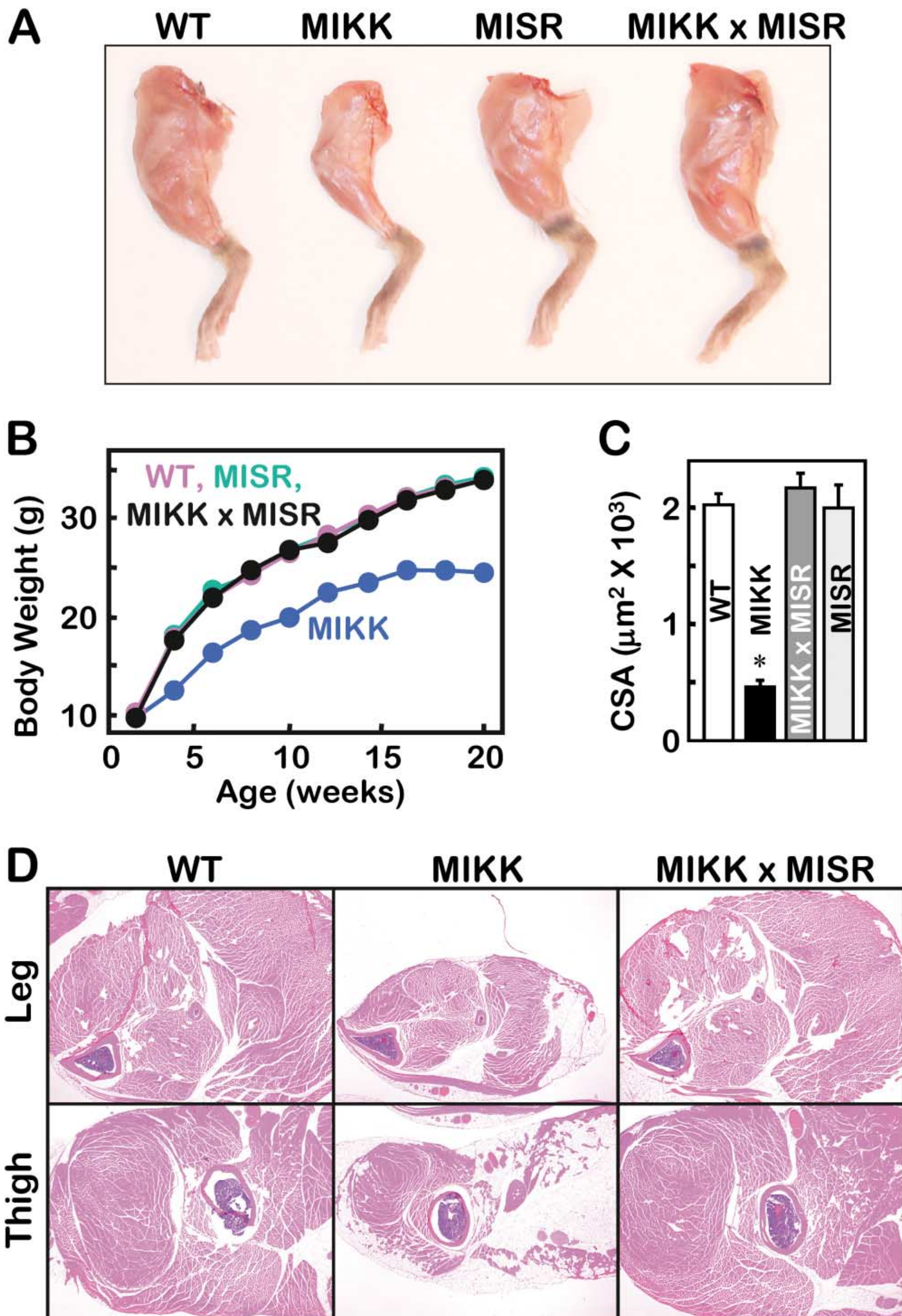

Figure 2. Reversal of the MIKK Phenotype by Transgenic Expression of IκBα Superrepressor

MIKK and MISR mice were crossed to create compound transgenic MIKK x MISR mice. (A) Skin was stripped from the hind limbs of 20-week-old mice for gross comparisons of muscle mass. (B) Body weights of wt (pink), MISR (green), and MIKK x MISR (black) are superimposed, whereas body weights of MIKK mice (blue) are distinctly reduced (n = 6 in each group). (C) Cross-sectional areas for individual EDL muscle fibers were measured in transverse frozen sections (n = 6 for each genotype; mean ± SEM; *$p < 10^{-8}$ versus wt). (D) H&E-stained transverse sections, taken at the midpoints of legs and thighs, were made from wt, MIKK, and MIKK x MISR mice.

are normal in terms of appearance, body weight (Figures 2A and 2B), individual muscle weight, and histology (data not shown). MIKK and MISR mice were crossed to determine whether the muscle loss phenotype was dependent on NF-κB activation. Concomitant muscle-specific expression of the IκB superrepressor in MIKK x MISR mice reduced NF-κB activity to levels seen in wt animals (Figure 1E), despite continued high-level IKKβ activity. Notably, the MIKK phenotype was completely reversed in MIKK x MISR mice (Figure 2). Body weight

(Figure 2B) and muscle mass were restored (Figures 2A and 2D), and histology of MIKK x MISR muscle was indistinguishable from wt controls (data not shown). While fiber size in MIKK mice was reduced to ~20% of that in wt mice, this parameter was also restored to normal levels in MIKK x MISR (Figure 2C). These data verify that the loss of muscle mass in MIKK mice is NF-κB dependent, as opposed to being mediated by IKKβ through an alternative pathway.

Pharmacological Reversal of the MIKK Phenotype
High-dose salicylates have been shown to inhibit IKKβ and NF-κB (Kopp and Ghosh, 1994; Yin et al., 1998; Yuan et al., 2001). We therefore asked whether salicylate treatment had an effect in MIKK mice. Two distinct protocols were followed, one to look at treatment and the other to look at prevention of the muscle wasting phenotype. The treatment protocol was initiated after weaning in 4-week-old affected mice. MIKK body weights increased with salicylate treatment (Figure 3A); after 6 months of therapy, body weight, muscle mass, and fiber size had approached normal levels (Figures 3B–3D). Salicylate therapy inhibited NF-κB activity in MIKK muscle by 77% (Figure 3E). For the prevention protocol, the same regimen was used, except mice were treated during gestation and until weaning, at which time the pups were treated with salicylate. Body weights and muscle mass were close to normal during the prevention protocol (Figure 3F), suggesting that earlier intervention affords an added benefit despite the fact that newborn muscle appears to be histologically normal. Much like IκBα expression, high-dose salicylate rescued the MIKK phenotype by inhibiting NF-κB signaling (Figure 3E).

Catabolism and Protein Turnover in MIKK Mice
Muscle wasting syndromes are catabolic and often accompanied by increases in resting energy expenditure and thermogenesis (Argiles and Lopez-Soriano, 1999). MIKK mice and wt littermates were studied for 68 hr in cages designed to measure a variety of metabolic parameters. Food and water consumption and activity levels were normal. However, O_2 consumption and CO_2 and heat production were significantly elevated in MIKK mice by 12%, 13%, and 17%, respectively (Supplemental Figure S2).

Muscle wasting syndromes are often associated with increases in circulating and excreted protein breakdown products (Jagoe and Goldberg, 2001). Concentrations of amino acids and their metabolites were elevated in MIKK mouse urine by an average of 45% (Supplemental Table S1). These findings suggest that the MIKK phenotype is associated with increased protein catabolism.

A protein breakdown assay using EDL muscles tested whether the catabolism was occurring in skeletal muscle and thus accounted for the apparent atrophy. Ex vivo tyrosine release increased 1.9- to 2.4-fold in muscles from 5- and 32-week- old MIKK mice (Figure 4A). A complementary protein synthesis assay revealed 2.3- to 2.5-fold increases in MIKK muscle synthesis (Figure 4B). Although the fold increases in protein breakdown and synthesis appeared to be balanced in these assays, the markedly smaller size of MIKK muscle fibers demonstrates that, at steady state in living animals, the net effect favors degradation. In fact, the proteasome inhibitor MG-132 reduced protein breakdown in EDL muscles of both MIKK and wt mice to similar levels (Figure 4A), suggesting that, in MIKK mice, increased protein degradation is largely mediated by ubiquitin- and proteasome-dependent pathways. Protein synthesis and breakdown rates were normal in soleus muscles of MIKK mice (data not shown). Muscle wasting upon in vivo activation of IKKβ and NF-κB thus appears to be mediated by ubiquitin-proteasome mechanisms. Our data is consistent with previous suggestions that ubiquitin-dependent proteolysis is involved in muscle atrophy (Jagoe and Goldberg, 2001; Glass, 2003; Li, 2003).

NF-κB Activates Proteolysis but Not Cytokine Signaling in Muscle
To further explore potential mechanisms for muscle wasting in MIKK mice, we asked whether cytokines, such as those typically driven by NF-κB in other tissues, were being produced in MIKK muscle. Quantitative RT-PCR analyses revealed normal muscle mRNA levels for many of these cytokines, including TNF-α, IL-6, IL-1β, IFN-γ, IL-2, IL-8, IL-10, LIF, and CNTF and their receptors, including TNF-α receptors 1 and 2, IL-1β receptors 1 and 2, IFN-γ receptor, and IL-6 receptors α and β (gp130) (Supplemental Table S2). Consistent with the mRNA data, circulating levels of TNF-α (wt 5.7 ± 0.4 versus MIKK 5.9 ± 0.5 pg/ml, $n = 8$, $p =$ NS), IL-6 (below detection) and IL-1β (wt 3.7 ± 0.4 versus MIKK 4.1 ± 0.6 pg/ml, $n = 8$, $p =$ NS) were normal in MIKK mice. These data suggest that, while NF-κB acts downstream of cachexia-inducing factors, in muscle, its activation is not sufficient to induce the transcription of cytokines reportedly linked to muscle wasting. This is in contradistinction to NF-κB's function in inflammation and innate immunity, where many cytokines activate NF-κB and many of the same cytokines and more are released in a positive feedback response (Van Antwerp et al., 1996; Baeuerle and Baltimore, 1996; Delhase et al., 1999; Rothwarf and Karin, 2000).

Gene microarray experiments were conducted to help determine the genes perturbed by increased NF-κB activity in the muscles of MIKK mice, and the results drew additional attention to elements of the proteasome degradation pathway. Subsequent RT-PCR experiments revealed a 3.3-fold increase in mRNA levels for *MuRF1* (Supplemental Table S2), a muscle-specific E3 ligase (Bodine et al., 2001; Glass, 2003), and 2.4- to 2.8-fold increases in mRNA for the *C2* and *C9* subunits of the proteasome (Supplemental Table S2). mRNA levels for other associated genes, including *ubiquitin*, *E2*(14KD) and *atrogin-1/MAFbx*, were normal. Message levels were normal as well for lysosomal and calcium-dependent proteases, including *calpains 1* and *2* and *cathepsins B* and *D* (Supplemental Table S1). In separate experiments, *MuRF1* message (Figure 4C) and protein (Figure 4D) levels were increased in MIKK mice and decreased in MISR mice, compared to wt controls. Elevated *MuRF1* message and protein levels were concordantly reduced in doubly transgenic MIKK x MISR mice (Figures 4C and 4D). To test whether *MuRF1* is a NF-κB target, we constructed a luciferase reporter assay using a 4.4 kB segment of the *MuRF1* promoter and transfected this

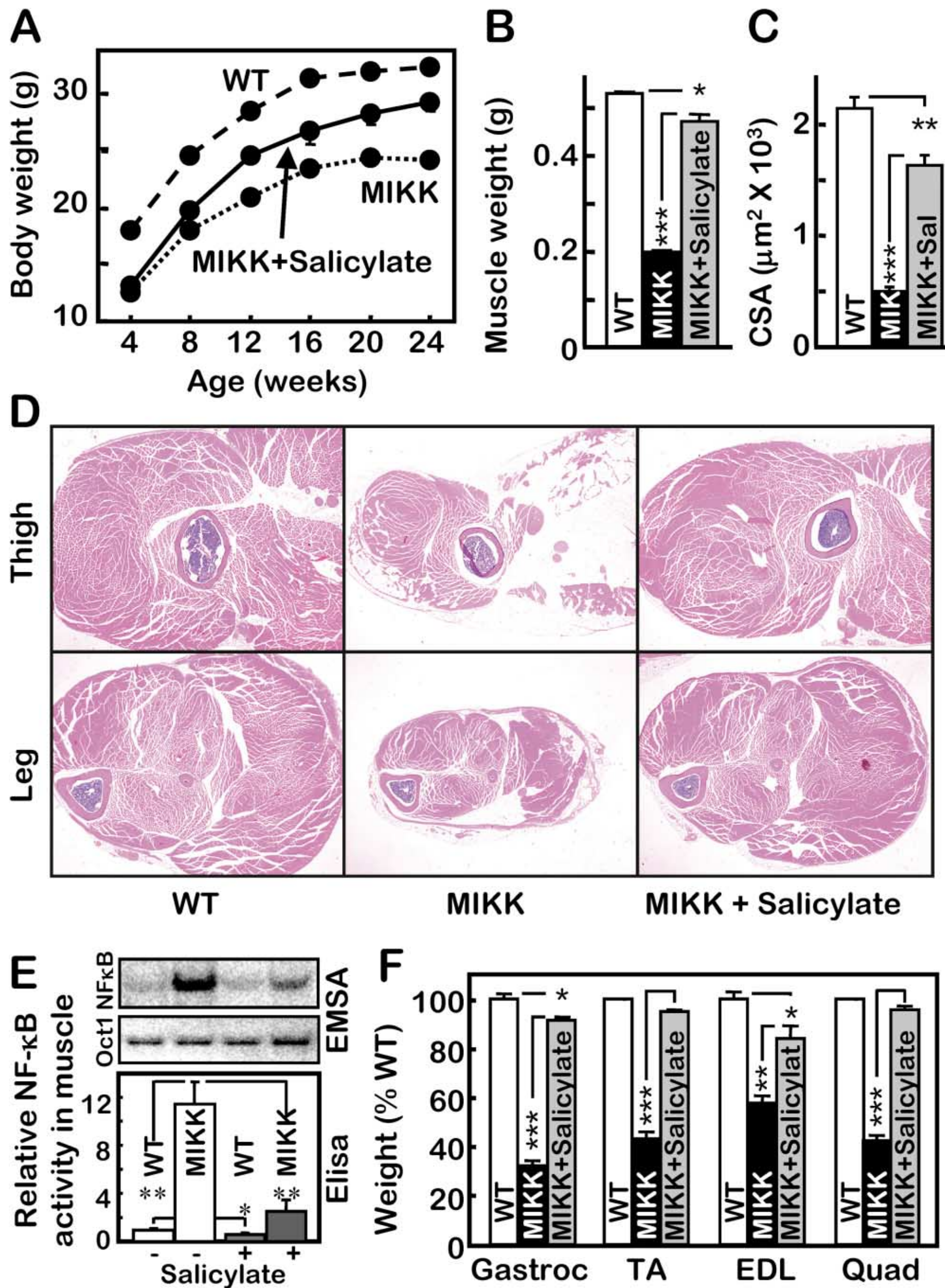

Figure 3. Reversal of the MIKK Phenotype using High-Dose Salicylate to Inhibit IKKβ/NF-κB

Salicylate was dissolved in the drinking water (6 mg/ml) and incorporated in the chow (500 mg/kg). Treatment protocol, (A) Body and (B) muscle weights (gastrocnemius + TA + EDL + quadriceps + biceps), (C) cross-sectional areas of EDL muscles, and (D) H&E-stained transverse sections of legs and thighs from 7-month-old mice (n = 6/group) treated with high-dose salicylate therapy that had been initiated at 4 weeks of age. (E) NF-κB activity was measured in gastrocnemius muscle lysates using EMSA and ELISA assays. Oct1 activity was measured as control transcriptional factors for all samples. Wild-type and MIKK mice had been treated for 6 months with oral salicylate. (F) Prevention protocol, weights of individual muscles from 6-month-old mice treated with high-dose salicylate initiated in utero (mothers and weaned offspring received salicylate in the water and food; n = 6; mean ± SEM). All panels, *$p < 0.05$, **$p < 0.001$, ***$p < 10^{-5}$.

into differentiated C2C12 myotubes. TNF-α or IL-1β stimulation or coexpression of constitutively active IKKβ increased transcriptional activity by 4.6-, 2.3-, and 1.7-fold, respectively (Figure 4E). Expression of the IκBα superrepressor supported the suggestion that *MuRF1* is an NF-κB target, as it reduced both basal and stimulated expression under each of the tested conditions (Figure 4E). These data fit recent observations showing that *MuRF1* mRNA is induced by IL-1β, sepsis, and reactive oxygen, all potential in vivo activators of NF-κB (Bodine et al., 2001; Wray et al., 2003; Li et al., 2003).

To determine whether MuRF1 mediates NF-κB-driven muscle wasting, we crossed MIKK and *MuRF1*$^{-/-}$ knockout mice (Bodine et al., 2001) to create MIKK x

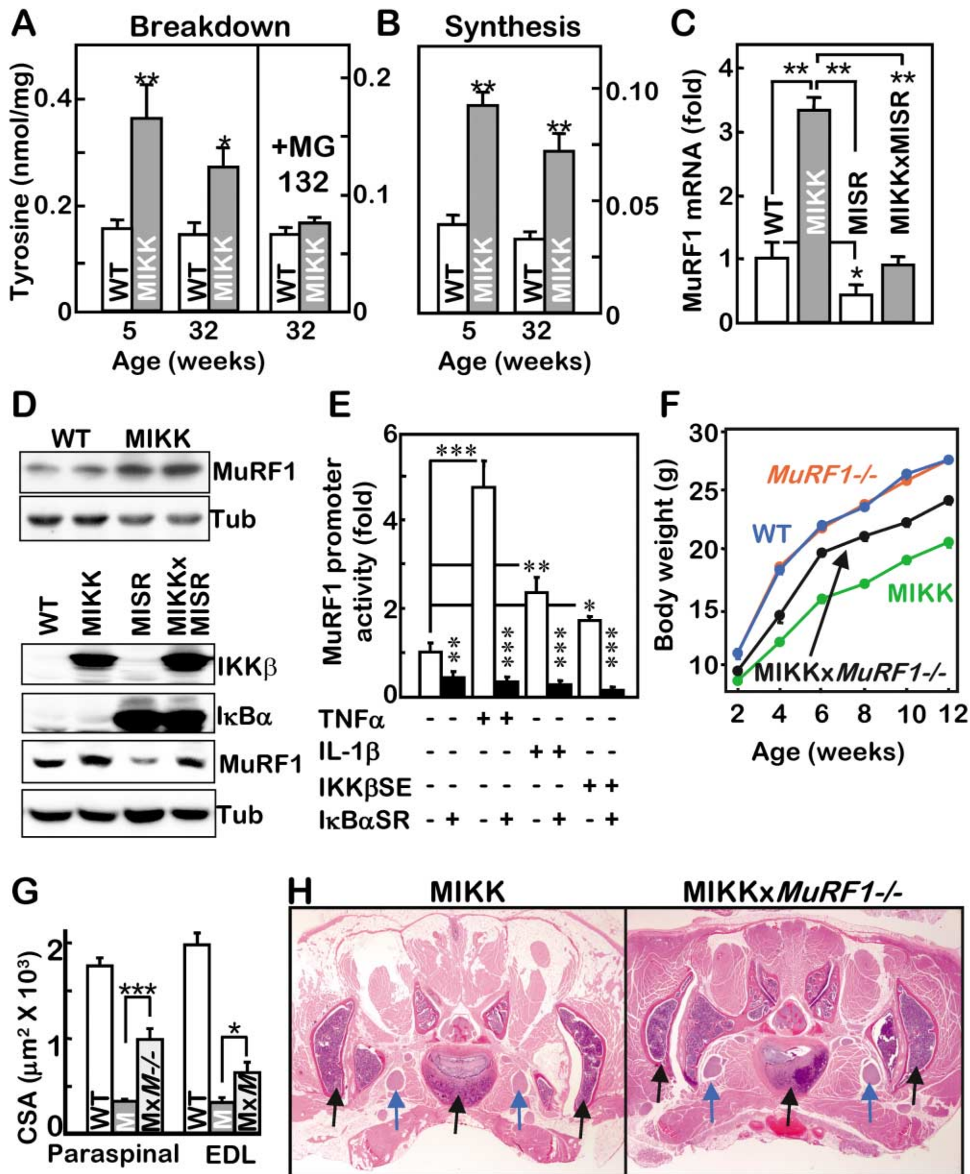

Figure 4. Ubiquitin-Dependent Proteolytic Pathway in MIKK Mice

Assays used isolated EDL muscles to simultaneously measure (A) protein breakdown and (B) protein synthesis (Tawa et al., 1997) (n = 6–7; *p < 0.05; **p < 0.01). The proteasome inhibitor MG-132 (10 μM) was added to the media in selected experiments. (C) Quantitative real-time RT-PCR was used to quantify MuRF1 mRNA in TA muscles of wt, MIKK, MISR, and MIKK x MISR (n = 6–7/group). (D) Western blot analyses of (upper) MuRF1 protein in gastrocnemius and (lower) IKKβ, IκBα, and MuRF1 in TA muscle (Tub = tubulin). (E) A reporter assay was developed using the promoter from MuRF1 linked to the luciferase gene. Differentiated C2C12 myotubes were cotransfected with the MuRF1 reporter, control PRL-TK, and either pCMV-IKKβ SS177/181EE (IKKβ SE), pCMV-IκBα SS32/36AA (IκBα SR), or empty vector and stimulated with cytokines. (F) MIKK and *MuRF1*$^{-/-}$ mice were crossed to obtain mice having the compound MIKK x *MuRF1*$^{-/-}$ genotype. Body weights of wt and *MuRF1*$^{-/-}$ mice were indistinguishable, whereas weights of MIKK x *MuRF1*$^{-/-}$ mice were intermediate between these and MIKK mice. (G) Cross-sectional areas of muscle fibers were measured in transverse sections of paraspinal and EDL muscles of wt, MIKK (M), and MIKK x *MuRF1*$^{-/-}$ (M x *M*$^{-/-}$) mice (n = 6/group). (H) Transverse sections show retroperitoneal muscles at the level of the pelvis. Black arrows point to the spine (midline) and pelvic bones (either side), and blue arrows point to sciatic nerves as landmarks (12.5× magnification). All panels, *p < 0.05, **p < 0.01, ***p < 0.001.

MuRF1$^{-/-}$ mice. Mice with the compound genotype had intermediate body weights between wt and MIKK, demonstrating an approximately 50% reversal of the muscle wasting phenotype by *MuRF1* deletion (Figure 4F). Rescue was greatest for axial trunk muscles and less for muscles of the limbs (Figures 4G and 4H). Cross-sectional areas of paraspinal muscle fibers in MIKK mice were 19% the size of wt fibers. Reductions in fiber size in MIKK x *MuRF1*$^{-/-}$ mice (55% of wt) were much less than in MIKK mice. Cross-sectional areas of EDL muscle fibers in MIKK mice were equivalently reduced to ~18% the size of wt fibers. However, the rescue was of a smaller magnitude, as cross-sectional areas of MIKK x *MuRF1*$^{-/-}$ EDL muscles were 32% of wt. The apparent

differences in rescue efficiency between trunk and peripheral muscles due to *MuRF1* deletion may be a reflection of developmental as well as functional differences between these muscle groups. The incomplete rescue seen in both axial and limb muscles demonstrates that NF-κB activates other atrophic pathways in addition to *MuRF1*.

NF-κB Blockade Rescues Muscle Wasting in Denervation and Cancer Cachexia

Since NF-κB activity has been reported to increase in muscle in response to immobilization (Hunter et al., 2002), we asked whether this was true as well in a related, denervation model of muscle atrophy and whether the reverse, NF-κB inhibition, might decrease muscle loss. NF-κB activity increased 9-fold in the hind limb muscles of wt mice 14 days after severing their sciatic nerves (Figure 5A). In contrast, NF-κB activity increased only 1.5-fold in the denervated muscle of MISR mice. Atrophy was readily apparent in denervated muscle, with mass decreased by 51% relative to sham-operated controls (Figure 5B). Fiber size (cross-sectional area) similarly decreased by 53% in denervated muscles (Figures 5C and 5D). Inhibition of NF-κB in MISR mice was accompanied by a partial rescue of the denervation-induced atrophy, including less loss of muscle mass (Figure 5B) and fiber size (Figures 5C and 5D) (38% $p < 0.05$ and 28% $p < 0.01$, respectively).

Similar studies were conducted using a mouse model for cancer cachexia to determine the extent to which NF-κB is involved in the pathogenesis of this disorder. Lewis lung carcinoma (LLC) cells are often used to create a model for cancer cachexia-induced muscle wasting in mice. Subcutaneous injection of LLC cells leads to the growth of large tumors at the injection sites and diffuse tumors in the lungs. NF-κB activity, increased 6-fold in the muscles of wt mice with tumors, was normal in MISR mice with similar tumor burdens (Figure 6A). Since no tumor could be found in the muscle itself, increased NF-κB activity was presumably due to the effects of circulating "cachexia" factor(s). Body weights typically begin to decrease within 1 week and continue to decrease over the subsequent week after tumor cell injection. Body weights of 8-month-old wt mice injected with LLC cells were decreased 6.6% on day 8, relative to uninjected controls, and were decreased 13.2% by day 12 (Figure 6B). In contrast, body weights of MISR littermates decreased 1.6% on day 8 and 6.7% on day 12, relative to uninjected MISR controls. The size and histology of the tumors at the injection sites (Figure 6F) and tumor burden in the lungs (data not shown) were essentially identical in wt and MISR mice, suggesting that the muscles of MISR mice were less responsive to the effects of the cachexia factor(s) in terms of both NF-κB activation and muscle wasting. This was further suggested using death as an endpoint, as all of the 2-month-old wt mice died within 28 days, whereas 40% of the MISR littermates survived to 30 days (at which point they were sacrificed) (Figure 6E). This was presumably due to the greater degree of muscle wasting, particularly in the respiratory muscles, of wt versus MISR mice. At day 12, gastrocnemius and TA muscles of wt mice had decreased in weight by 28%, compared to a 15% decrease in muscle mass of MISR mice (Figure 6C). This was manifested by a 33% reduction in cross-sectional fiber area in wt mice, compared to a 15% reduction in cross-sectional fiber area in littermate MISR mice (Figures 6D and 6F). Selective NF-κB blockade in muscle thus decreases muscle wasting and prolongs survival in this mouse model of cancer cachexia.

Relationships between Muscle NF-κB and Insulin Resistance

We have shown previously that activation of IKKβ and NF-κB promotes insulin resistance, whereas their inhibition improves insulin sensitivity (Yuan et al., 2001). We therefore used MIKK and MISR mice to ask whether muscle IKKβ/NF-κB modulates insulin sensitivity. MISR mice are normal in terms of insulin sensitivity, glucose tolerance, and lipid levels. Fasting blood glucose (102 ± 5.6 mg/dl) and insulin (0.77 ± 0.12 ng/ml) levels in MISR mice are similar to wt littermates (97 ± 7.3 mg/dl and 0.81 ± 0.19 ng/ml, respectively). Glucose concentrations during glucose tolerance testing were similarly matched between MISR mice and wt littermates (AUC: 736 ± 50 versus 787 ± 94 mg/dl·h). Free fatty acid levels were equivalent, as well (wt, 1.64 ± 0.21; MISR, 1.48 ± 0.33 mEq/l). Importantly, NF-κB inhibition in MISR mice afforded no protection against the development of obesity-induced insulin resistance. After 3 months of a high-fat diet fasting blood glucose (120 ± 17 versus 115 ± 14 mg/dl) and insulin (1.4 ± 0.7 versus 1.2 ± 0.8 ng/ml) concentrations were similar in MISR mice versus wt controls, and glucose concentrations following a glucose challenge were similar in high-fat-fed MISR and wt mice (AUC: 972 ± 130 versus 1019 ± 105 mg/dl·h, respectively).

Activation of NF-κB in skeletal muscle does not cause MIKK mice to become insulin resistant. Fasting blood glucose and insulin concentrations in 12- to 15-week-old MIKK mice (92 ± 6.6 mg/dl and 0.37 ± 0.07 ng/ml, respectively) and wt littermate controls (95 ± 3.8 mg/dl and 0.34 ± 0.05 ng/ml) were similar, as were glucose levels during glucose tolerance testing (AUC: MIKK, 708 ± 122 mg/dl·h; wt, 671 ± 98 mg/dl·h). Ex vivo glucose uptake in isolated EDL muscles of MIKK and wt mice was comparable (data not shown). In contrast, serum-free fatty acid concentrations were elevated in MIKK mice (3.0 ± 0.3 mEq/l) relative to wt littermates (1.8 ± 0.2 mEq/l; $p < 0.01$). The known association between cachexia and elevations in circulating lipids may explain these findings (Rossi et al., 1995; Lopez-Soriano et al., 1996; Argiles and Lopez-Soriano, 1999). We have concluded, since insulin sensitivity is not altered in MIKK or MISR mice, under both basal and provocative conditions, that IKKβ, NF-κB, and MuRF1 mediate muscle wasting without being directly involved in the development of insulin resistance in this tissue.

Discussion

NF-κB was activated or inhibited selectively in the skeletal muscle of transgenic mice through expression of either constitutively active IKKβ or a dominant inhibitory form of IκBα. These mice are referred to as MIKK (muscle-specific expression of IKK) or MISR (muscle-specific

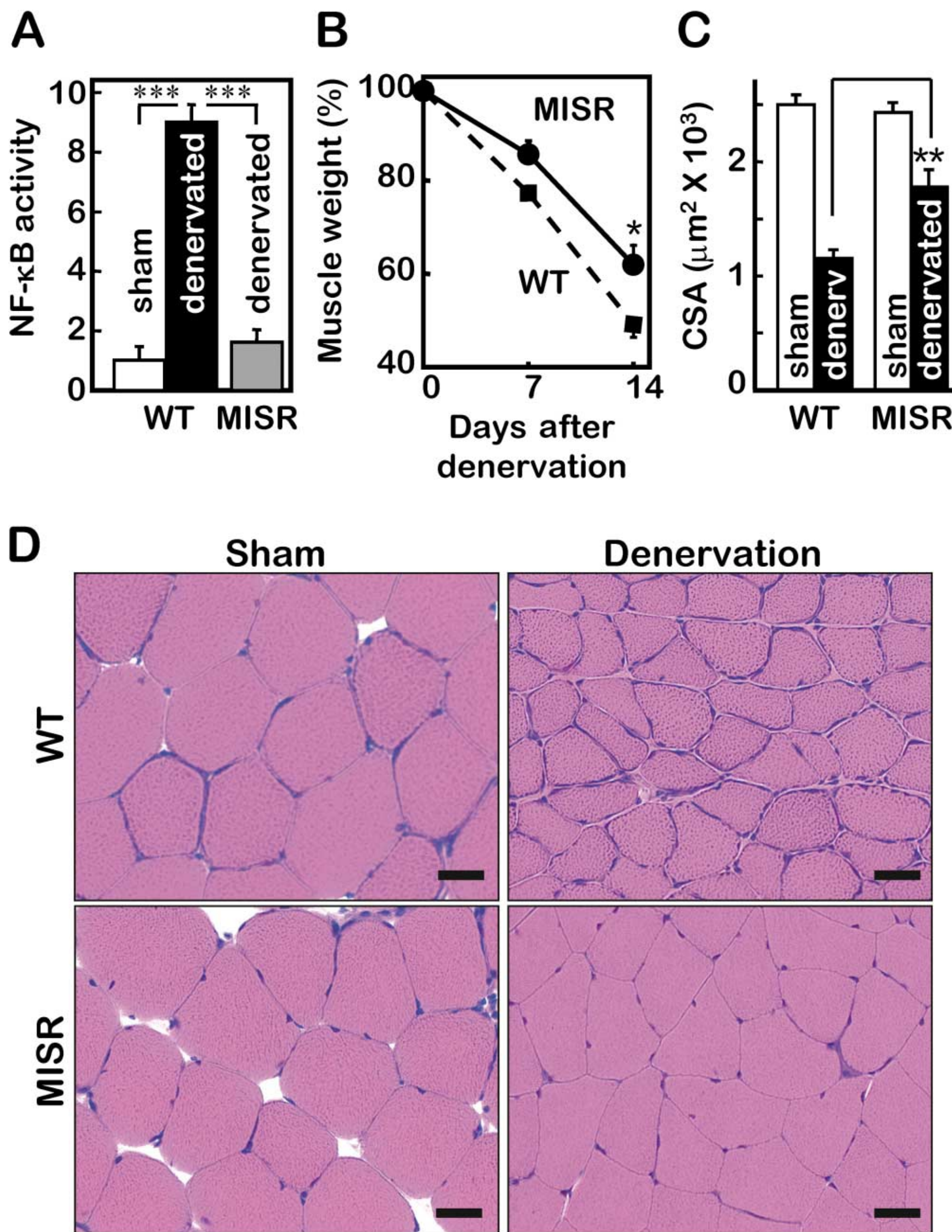

Figure 5. Protection against Denervation-Induced Muscle Atrophy by NF-κB Inhibition

(A) ELISA assays were used to measure NF-κB activity in wt (sham and denervated) and MISR (denervated) muscle. (B) Gastrocnemius and TA muscles were isolated and weighed after the sciatic nerves of MISR and wt mice had been severed (n = 4–6/group). Data were plotted as weight denervated muscle divided by weight sham-operated muscle × 100%. (C) Cross-sectional fiber areas were determined in transverse sections of gastrocnemius muscle from denervated or sham-operated wt and MISR mice. (D) H&E-stained transverse sections of frozen gastrocnemius muscle are shown at 200× magnification (solid bars = 35 μm). Data represent mean ± SEM; all panels, *$p < 0.05$; **$p < 0.01$; ***$p < 0.001$.

expression of IκB superrepressor), respectively. Analyses of MIKK mice demonstrated for the first time that activation of the IKKβ/NF-κB pathway is sufficient to induce serious skeletal muscle atrophy reminiscent of that seen during cachexia, cancer, AIDS, denervation, and immobilization.

Several parameters of atrophy were identified in MIKK mice. First, protein catabolism was elevated, as measured by increases in in vivo amino acid excretion and tyrosine turnover in isolated muscles. Second, the increased catabolism occurred via the ATP-dependent, ubiquitin/proteasome pathway, since a pharmacological inhibitor of the proteasome, MG132, returned protein turnover to wild-type levels in muscles from MIKK mice. It has been previously reported that atrophy is mediated in large part by the ubiquitin proteasome pathway (Lecker et al., 1999). Third, expression of the ubiquitin ligase, *MuRF1*, a high-fidelity marker of muscle atrophy

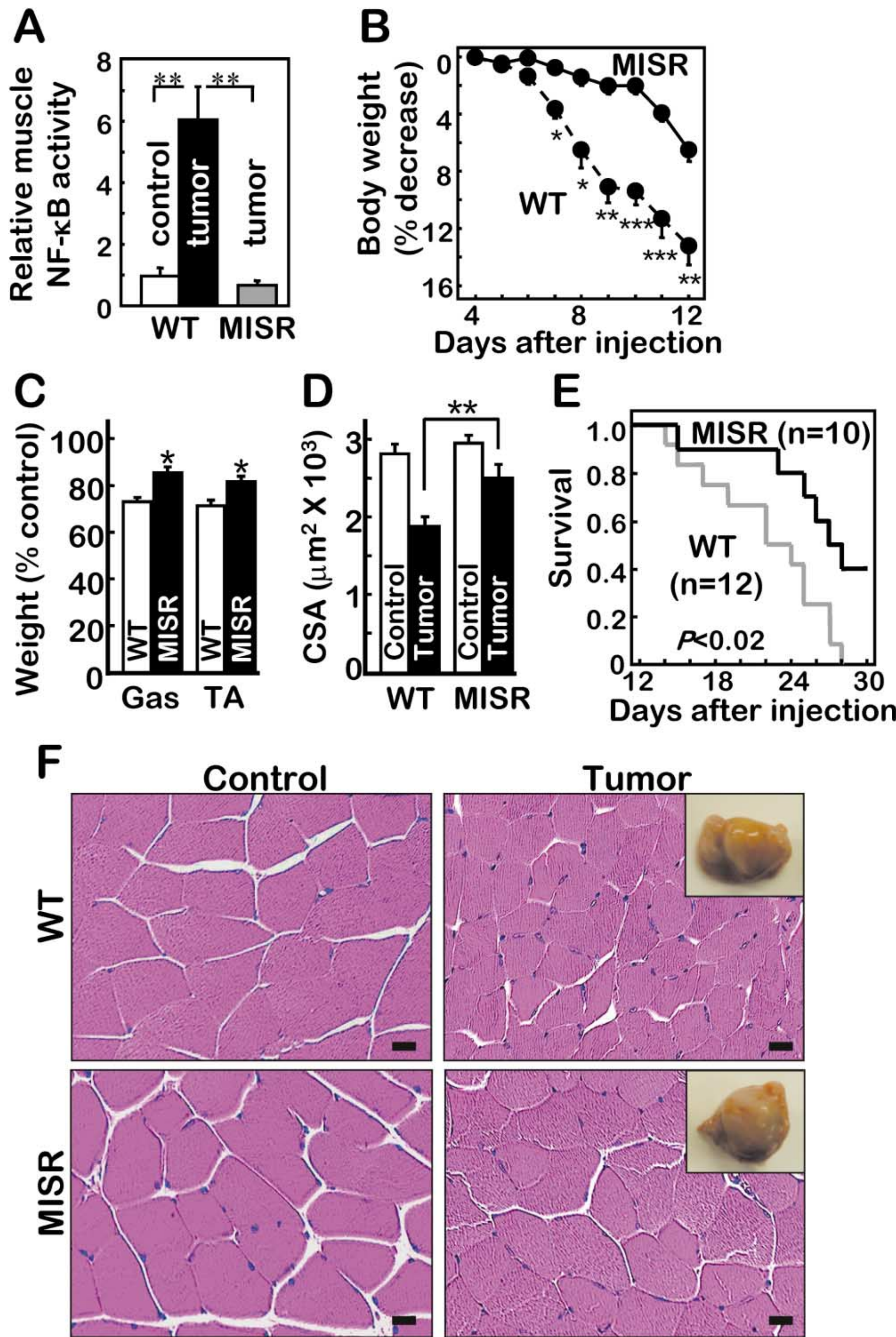

Figure 6. NF-κB Inhibition Protects against Cancer-Induced Muscle Atrophy

Eight-month old mice were injected with LLC cells to induce tumor growth. (A) NF-κB activity was measured by ELISA assay in wt and MISR muscle 12 days after subcutaneous injection of LLC cells. (B) Mice were weighed each day after injection of the LLC cells ($n = 6$); data are reported relative to uninjected controls. (C) Weights of gastrocnemius (Gas) and TA muscles and (D) cross-sectional fiber areas were measured in transverse sections of gastrocnemius 12 days after injection of LLC cells. (E) Survival curves for 2-month-old wt and MISR mice after injection with identical numbers of LLC cells ($n = 10$–12; p value determined using a Wilcoxon test). (F) H&E-stained transverse sections of gastrocnemius muscle are shown at 200× magnification (Solid bars = 35 μm). (Inserts) Tumors removed from the primary injection sites (diameter ~1.5 cm). Data represent mean ± SEM; all panels, $^{*}p < 0.05$; $^{**}p < 0.01$; $^{***}p < 0.001$.

(Bodine et al., 2001; Wray et al., 2003; Li et al., 2003), was shown to be greater in MIKK muscle relative to levels seen in wild-type muscle. Fourth, and perhaps most strikingly, muscle mass was significantly reduced in MIKK mice relative to wild-type controls, indicating that increased catabolism results in phenotypic atrophy and is not sufficiently compensated by an increase in protein synthesis. The reduction in mass comes as a result of reduced cross-sectional area of individual muscle fibers, as opposed to changes in fiber number. This is the situation seen in clinical settings of atrophy. In the quadriceps muscle of older MIKK animals, there is some replacement of muscle with adipose tissue, as occurs in paraplegic patients after long-term denervation-induced skeletal muscle atrophy (Mora, 1989).

When MIKK and MISR mice were crossed, the atrophic phenotype was reversed, thus demonstrating that the loss of muscle mass was not only induced by activation of NF-κB but could be blocked by genetic inactivation of NF-κB at the level of IκBα. NF-κB has previously been demonstrated to be activated upon treatment of C2C12 cells with the cachectic factor TNFα (Guttridge et al., 2000; Li and Reid, 2000; Langen et al., 2001; Ladner et al., 2003) and during immobilization-induced decreases in muscle mass (Hunter et al., 2002). Also, a previous in vitro study demonstrated that overexpression of IκBα could block loss of myosin in TNFα-treated C2C12 myotubes (Ladner et al., 2003). The current study is consistent with the previous data and provides the first in vivo evidence that blockade of NF-κB can block atrophy. In addition to genetic complementation, a pharmacological inhibitor of the NF-κB pathway, sodium salicylate, was sufficient to partially suppress the atrophic phenotype in MIKK mice. High doses of sodium salicylate were previously reported to block IKKβ and NF-κB (Kopp and Ghosh, 1994; Yin et al., 1998; Yuan et al., 2001).

To assess the physiologic role of the NF-κB pathway in clinically relevant settings, MISR mice were subjected to both denervation- and tumor-induced atrophy. In both conditions, blockade of the NF-κB pathway resulted in a significantly reduced loss of muscle mass as compared to that observed in wild-type mice undergoing the same perturbations. These data suggest that the NF-κB pathway may be one of the long-sought, critical triggers induced by atrophic stimuli, upstream of the proteolytic pathways that mediate catabolism. One indication that this may be the case is that activation of NF-κB in MIKK mice resulted in increased expression of the E3 ubiquitin ligase *MuRF1*. MuRF1 is upregulated in at least ten different settings of skeletal muscle atrophy (Bodine et al., 2001; Wray et al., 2003; Glass, 2003). Further, in *MuRF1*$^{-/-}$ animals, the degree of atrophy is reduced relative to wild-type controls (Bodine et al., 2001), reminiscent of the sort of reduction seen here in MISR animals. When MIKK mice were crossed into a *MuRF1*$^{-/-}$ background, there was a significant reduction in muscle loss, though less than that seen when MIKK mice were crossed with MISR mice. Although MuRF1 is therefore not the only critical mediator of muscle atrophy to be activated by the NF-κB pathway, its ablation, even in the setting of continued activation of NF-κB, partially ameliorates the atrophic phenotype. With this data, a stepwise IKKβ/NF-κB/MuRF1 signaling pathway can now be proposed (Figure 7) in which atrophic stimuli such as denervation and tumor-induced factors activate NF-κB, which in turn results in upregulation of *MuRF1* as well as other critical pathways which have yet to be elucidated.

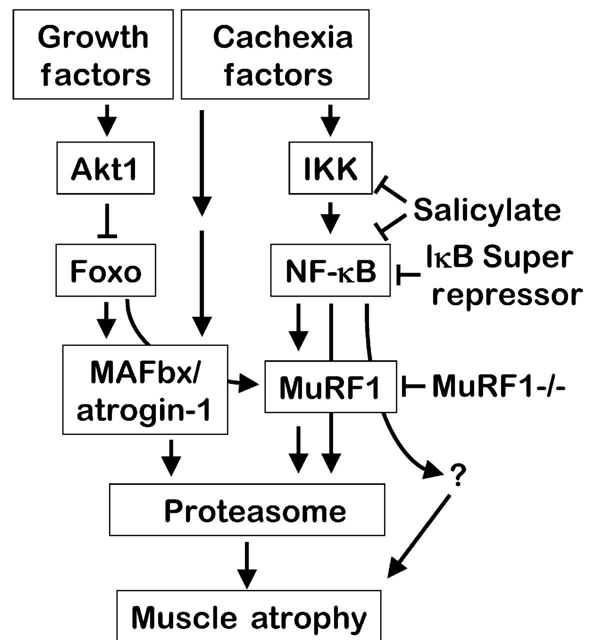

Figure 7. Proposed Pathways that Integrate Muscle Hypertrophy and Atrophy

Recent findings demonstrated the involvement of the Foxo family of transcription factors to be required for the activation of MuRF1 and MAFbx/Atrogin-1 (Sandri et al., 2004; Stitt et al., 2004). By activating Akt, growth factors such as IGF-1, which induces hypertrophy, block the induction of *MuRF1* and *MAFbx/Atrogin-1* mRNA. Activation of the IKKβ/NF-κB axis, which is induced by cachexia, is required to activate MuRF1 and is sufficient to induce muscle atrophy (this work). The IKKβ/NF-κB/MuRF1 pathway may be suppressed at multiple steps, including salicylate inhibition of IKKβ and expression of the IκBα superrepressor to inhibit NF-κB, and by genetic ablation of *MuRF1*.

It is noteworthy that a second ubiquitin ligase, alternatively named MAFbx (Bodine et al., 2001) or atrogin-1 (Gomes et al., 2001), was neither activated nor inhibited in the MIKK animals. MAFbx had been shown previously to be activated in multiple models of atrophy and often at levels greater than observed for MuRF1. The MIKK animals are the first setting of atrophy to be reported where MAFbx is not upregulated. Thus, MAFbx upregulation is not required for NF-κB-induced muscle loss. However, given the diverse settings that do result in MAFbx/atrogin upregulation, the implication is that a second, parallel pathway, distinct from NF-κB activation, is usually induced during atrophy. This idea is also consistent with the MISR data, which shows significant but partial amelioration of denervation and tumor-induced atrophy, indicating that the IKKβ/NF-κB pathway is a critical mediator of muscle loss in these clinical settings but not the only mediator.

Many of what would typically be considered NF-κB target genes were not activated in muscles of MIKK mice. Functions have been studied most extensively in

immune and inflammatory cells and liver, where NF-κB orchestrates the synthesis of a host of mediators of cell survival and innate immune and inflammatory responses. Despite high-level activation of NF-κB in muscles of MIKK mice, none of the typical cytokines, chemokines, or associated receptors was upregulated as would be expected in these other cell types. While NF-κB may be activated in muscle by certain proinflammatory and cachexia-inducing cytokines, it must not drive their synthesis as in other tissues. Therefore, NF-κB has dramatically different functions in distinct tissues. In muscle, the catabolic actions of NF-κB provide a mechanism for the sustained production of amino acids to be used as an energy source for other tissues. While this may be a normal physiological response, for example, during starvation, NF-κB activation in muscle appears to have deleterious and potentially disastrous consequences under pathological conditions.

It is of further interest to find signaling pathways that could dominantly suppress activation of NF-κB in skeletal muscle, since activation of those pathways could potentially help in suppressing atrophy. It was very recently reported that activation of the Akt kinase, which was previously shown to cause skeletal muscle hypertrophy via upregulation of protein synthesis pathways, could also dominantly suppress upregulation of both *MuRF1* and *MAFbx* during atrophy (Sandri et al., 2004; Stitt et al., 2004). Akt has been shown to activate NF-κB in various cell types. However, data reported here in conjunction with the Akt studies would seem to call into question whether Akt activates NF-κB in muscle, or at least suggests future studies focusing on an assessment of the Akt/NF-κB pathway in skeletal muscle.

The discovery that NF-κB activation is sufficient to cause skeletal muscle atrophy in vivo and that blockade of the NF-κB pathway can ameliorate atrophy suggests a new set of drug targets for clinical intervention during cachexia, cancer, AIDS, and other settings of atrophy. For example, the inhibition of atrophy with high doses of sodium salicylate suggests that more specific inhibitors of IKKβ might be useful to block atrophy—sodium salicylate itself has a range of other targets, and the high doses of it required for IKKβ inhibition are not well tolerated due to side effects. MuRF1 has already been suggested as a novel clinical target, and the data in this study help to put the previous findings in a larger signaling context. Further study of the IKKβ/NF-κB/MuRF1 pathway will help to uncover other clinically useful targets. This is critically important, because unfortunately, there are currently no drugs approved for the treatment of skeletal muscle atrophy.

Experimental Procedures

Transgenic Mice

cDNAs encoding Flag-tagged full-length IKKβ SS177/181EE (constitutively active) or HA-tagged full-length IκBα SS32/36AA (superrepressor) were subcloned into a truncated β-globin expression vector (Supplemental Figure S1A). A 3.3 kb fragment of DNA isolated from the mouse MCK promoter was subcloned upstream from exon 1 of the β-globin cassette (Donoviel et al., 1996). Microinjected mouse oocytes were introduced into pseudopregnant females. Transgenic offspring were identified originally by Southern analyses, and subsequent genotyping was by PCR. At least two independent lines were obtained for both MIKK and MISR mice, and each had the same phenotype.

Histology and Blood/Urine Chemistry

Cryostat and paraffin sections were stained with hematoxylin and eosin using standard techniques. Cross-sectional areas were determined for at least 50 fibers/animal, and six to ten animals were analyzed for each determination. NIH Image 1.6 software was used for the analyses. Fiber numbers in EDL muscle were counted in the entire cross-section ($n = 6$ animals/group). Nuclei were counted in similar sections of EDL muscle and normalized for fiber number ($n = 6$ animals/group). Plasma creatine kinase activity was determined using the EC 2.7.3.2 UV test kit (Sigma). Circulating cytokines were measured using Luminex assays (Linco).

NF-κB Assays

Nuclear proteins were isolated from gastrocnemius muscle using a combination of mechanical and osmotic disruption as described (Kumar and Boriek, 2003). Electrophoretic mobility shift assays (EMSA, Promega) were conducted with ^{32}P-labeled double-stranded oligonucleotides having consensus recognition sequences for NF-κB (5′-AGTTGA**GGGGACTTTCCC**AGG-3′) or Oct-1 (5′-TGTCGA**AT GCAAAT**CACTAGAA-3′); unlabeled probe was added to negative controls. Protein-DNA complexes were separated using nondenaturing PAGE. Similar extracts were used for ELISA assays of NF-κB activity, using immobilized κB binding motifs (GGGGACTTTCCC) in a 96-well format (BD Biosciences) (Fiorucci et al., 2002). Bound protein, recognized using anti-NF-κB p65 and IgG-HRP as primary and secondary antibodies, respectively, was quantified colorimetrically.

Kinase Assays

Kinase activity was assessed in immune complexes precipitated from muscle lysates. For measurements of IKK activity, recombinant GST-IκBα was used as a substrate for kinase activity precipitated with protein A Sepharose-immobilized anti-IKKγ (Pharmingen). To quantify p38 MAP kinase activity, GST-ATF2 (Santa Cruz) served as a substrate for kinase activity associated with anti-p38 (Santa Cruz). Proteins phosphorylated in the presence of [γ-^{32}P]ATP (20 μM) were separated by SDS/PAGE, and incorporated radioactivity was quantified using a phosphorimager (Storm, Molecular Dynamics).

Ex Vivo Determinations of Protein Turnover and Fiber Size and Contractility

EDL or soleus muscles were secured to inert supports for the simultaneous measurement of protein synthesis and degradation (Tawa et al., 1997). For selected measurements, muscles were incubated in media supplemented with 0.5 mM cycloheximide, to suppress protein synthesis; or 10 μM MG-132, 25 μM E-64, or 10 mM methylamine, to suppress proteasomal, lysosomal, or Ca^{2+}-dependent proteolysis, respectively (Tawa et al., 1997). For assessments of fiber size and contractile function, single, chemically skinned fibers were isolated from TA and soleus muscles and analyzed at 15°C as described (Larsson and Moss, 1993).

Cell Culture

C2C12 cells were cultured in DMEM supplemented with 5 mM glucose, 20% fetal bovine serum (FBS), 2 mM glutamine, and penicillin/streptomycin. Upon reaching confluence, cells were cultured in DMEM containing 25 mM glucose, 2% horse serum, 2 mM glutamine, and penicillin/streptomycin. HEK 293 cells were cultured in DMEM containing 25 mM glucose, 10% FBS, 2 mM glutamine, and penicillin/streptomycin. All cells were maintained at 37°C under 7.5% CO_2.

MuRF1 and NF-κB Reporter Assays

A 4.4 kB fragment of the mouse MuRF1 promoter was subcloned into the pGL3 firefly luciferase vector (Promega). C2C12 myotubes were cotransfected (Fugene, Roche) with pGL3-MuRF1, the control *Rellina* luciferase vector pRL-TK, and matched amounts of pCMV-empty, pCMV-IKKβSE, and/or pCMV-IκBαSR. HEK 293 cells were cotransfected with an NF-κB luciferase reporter provided by Dr. Gilmore (Sylla et al., 1998) and pCMV-IKKβSE and pCMV-IκBαSR. C2C12 myotubes or HEK 293 cells were cultured overnight in DMEM lacking serum and treated for 90–120 min with 6 nM TNF-α (Calbio-

chem) or IL-1β (R&D). Luciferase expression was quantified using a Dual-Luciferase Reporter Assay (Promega).

Western Blotting

Animal tissues were homogenized and incubated for 60 min at 4°C in lysis buffer, samples were separated by SDS/PAGE, and separated proteins were transferred to nitrocellulose or PVDF membranes and identified by immunoblotting. Primary antibodies included monoclonal anti-Flag (Strategene), anti-HA (Cell Signaling), anti-myosin type I and anti-myosin type II (Novocastra), anti-tubulin (Santa Cruz), anti-IKKγ (PharMingen), rabbit anti-IKKβ, anti-IKKα, anti-IκBα, (Santa Cruz), anti-α-actinin 3 (provided by Dr. Alan Beggs, Children's Hospital), and anti-MuRF1 (Bodine et al., 2001). Secondary antibodies included GFP- and rodamine-conjugating anti-mouse and anti-rabbit antibodies (Jackson ImmunoResearch) and HRP-conjugated anti-rabbit and anti-mouse antibodies (Pierce).

Quantitative Real-Time RT-PCR

Total RNA was extracted from mouse tissues or cultured cells using TRIzol (Invitrogen), and cDNA was synthesized using oligo (dT) primers with the Advantage RT-for-PCR Kit (BD Biosciences). Primers spanned intronic regions to generate 300–400 bp PCR products. PCR amplifications were quantified using the SYBRGreen PCR Master Mix (Applied Biosystems). Results were normalized against tubulin binding protein (TBP) and GAPDH gene expression.

Denervation and Cancer Cachexia

Right sciatic nerves were severed in 16-week-old anaesthetized MISR mice and wt controls. Left sciatic nerves were exposed but not severed to serve as sham-operated controls. Mice were sacrificed after 7 or 14 days, and individual muscles were weighed. For the cancer cachexia model, Lewis lung carcinoma (LLC) cells (ATCC; 5×10^6) were injected subcutaneously into the flanks of 8-month-old C57Bl/6 mice. Mice were weighed daily and sacrificed 12 days after injection. For survival studies, LLC cells were injected into the flanks of 2-month-old C57Bl/6 mice.

Statistical Analyses

Data are presented as mean ± SEM. Statistical significance was determined using unpaired Student's t tests.

Acknowledgments

We dedicate this manuscript to the memory of our friend and colleague, Valerie Fanikos. We wish to thank Dr. A. Beggs (Children's Hospital) and D. Guttridge (Ohio State University) for helpful discussions and advice; and D. Sanoudou, M. Fareed, G. Krishnan, and members of the Shoelson Lab including M. Yuan, Y. Guo, E. Werner, and L. Hansen for technical assistance. D.C. was supported by a Mentor-Based postdoctoral fellowship from the American Diabetes Association (S.E.S.). These studies were funded by NIH grants DK45943 (S.E.S.), DK51729 (S.E.S.), and DK36836 (Joslin DERC); and the Helen and Morton Adler Chair (S.E.S.). Regeneron conducts research and holds patents on intellectual property relating to the molecular mechanisms of muscle wasting.

Received: April 5, 2004
Revised: August 31, 2004
Accepted: September 2, 2004
Published: October 14, 2004

References

Argiles, J.M., and Lopez-Soriano, F.J. (1999). The role of cytokines in cancer cachexia. Med. Res. Rev. *19*, 223–248.

Baeuerle, P.A., and Baltimore, D. (1996). NF-κB: ten years after. Cell *87*, 13–20.

Bodine, S.C., Latres, E., Baumhueter, S., Lai, V.K., Nunez, L., Clarke, B.A., Poueymirou, W.T., Panaro, F.J., Na, E., Dharmarajan, K., et al. (2001). Identification of ubiquitin ligases required for skeletal muscle atrophy. Science *294*, 1704–1708.

Carpenter, S., and Karpati, G. (2001). Pathology of Skeletal Muscle (Oxford: Oxford University Press).

Coletti, D., Yang, E., Marazzi, G., and Sassoon, D. (2002). TNFα inhibits skeletal myogenesis through a PW1-dependent pathway by recruitment of caspase pathways. EMBO J. *21*, 631–642.

Delhase, M., Hayakawa, M., Chen, Y., and Karin, M. (1999). Positive and negative regulation of IκB kinase activity through IKKβ subunit phosphorylation. Science *284*, 309–313.

Donoviel, D.B., Shield, M.A., Buskin, J.N., Haugen, H.S., Clegg, C.H., and Hauschka, S.D. (1996). Analysis of muscle creatine kinase gene regulatory elements in skeletal and cardiac muscles of transgenic mice. Mol. Cell. Biol. *16*, 1649–1658.

Fang, C.H., Li, B.G., Tiao, G., Wang, J.J., Fischer, J.E., and Hasselgren, P.O. (1998). The molecular regulation of protein breakdown following burn injury is different in fast- and slow-twitch skeletal muscle. Int. J. Mol. Med. *1*, 163–169.

Fiorucci, S., Antonelli, E., Distrutti, E., Del Soldato, P., Flower, R.J., Clark, M.J., Morelli, A., Perretti, M., and Ignarro, L.J. (2002). NCX-1015, a nitric-oxide derivative of prednisolone, enhances regulatory T cells in the lamina propria and protects against 2,4,6-trinitrobenzene sulfonic acid-induced colitis in mice. Proc. Natl. Acad. Sci. USA *99*, 15770–15775.

Fong, Y., Moldawer, L.L., Marano, M., Wei, H., Barber, A., Manogue, K., Tracey, K.J., Kuo, G., Fischman, D.A., and Cerami, A. (1989). Cachectin/TNF or IL-1α induces cachexia with redistribution of body proteins. Am. J. Physiol. *256*, R659–R665.

Glass, D.J. (2003). Signalling pathways that mediate skeletal muscle hypertrophy and atrophy. Nat. Cell Biol. *5*, 87–90.

Gomes, M.D., Lecker, S.H., Jagoe, R.T., Navon, A., and Goldberg, A.L. (2001). Atrogin-1, a muscle-specific F-box protein highly expressed during muscle atrophy. Proc. Natl. Acad. Sci. USA *98*, 14440–14445.

Guttridge, D.C., Mayo, M.W., Madrid, L.V., Wang, C.Y., and Baldwin, A.S., Jr. (2000). NF-κB-induced loss of MyoD messenger RNA: possible role in muscle decay and cachexia. Science *289*, 2363–2366.

Hunter, R.B., Stevenson, E., Koncarevic, A., Mitchell-Felton, H., Essig, D.A., and Kandarian, S.C. (2002). Activation of an alternative NF-κB pathway in skeletal muscle during disuse atrophy. FASEB J. *16*, 529–538.

Jagoe, R.T., and Goldberg, A.L. (2001). What do we really know about the ubiquitin-proteasome pathway in muscle atrophy? Curr. Opin. Clin. Nutr. Metab. Care *4*, 183–190.

Kopp, E., and Ghosh, S. (1994). Inhibition of NF-κB by sodium salicylate and aspirin. Science *265*, 956–959.

Kumar, A., and Boriek, A.M. (2003). Mechanical stress activates the NF-κB pathway in skeletal muscle fibers: a possible role in Duchenne muscular dystrophy. FASEB J. *17*, 386–396.

Ladner, K.J., Caligiuri, M.A., and Guttridge, D.C. (2003). Tumor necrosis factor-regulated biphasic activation of NF-κB is required for cytokine-induced loss of skeletal muscle gene products. J. Biol. Chem. *278*, 2294–2303.

Langen, R.C., Schols, A.M., Kelders, M.C., Wouters, E.F., and Janssen-Heininger, Y.M. (2001). Inflammatory cytokines inhibit myogenic differentiation through activation of NF-κB. FASEB J. *15*, 1169–1180.

Larsson, L., and Moss, R.L. (1993). Maximum velocity of shortening in relation to myosin isoform composition in single fibres from human skeletal muscles. J. Physiol. *472*, 595–614.

Lecker, S.H., Solomon, V., Mitch, W.E., and Goldberg, A.L. (1999). Muscle protein breakdown and the critical role of the ubiquitin-proteasome pathway in normal and disease states. J. Nutr. *129*, 227S–237S.

Li, Y.P. (2003). TNF-α is a mitogen in skeletal muscle. Am. J. Physiol. *285*, C370–C376.

Li, Y.P., and Reid, M.B. (2000). NF-κB mediates the protein loss induced by TNF-α in differentiated skeletal muscle myotubes. Am. J. Physiol. *279*, R1165–R1170.

Li, Y.P., Chen, Y., Li, A.S., and Reid, M.B. (2003). Hydrogen peroxide stimulates ubiquitin-conjugating activity and expression of genes for specific E2 and E3 proteins in skeletal muscle myotubes. Am. J. Physiol. *285*, C806–C812.

Ling, L., Cao, Z., and Goeddel, D.V. (1998). NF-κB-inducing kinase

activates IKK-α by phosphorylation of Ser-176. Proc. Natl. Acad. Sci. USA *95*, 3792–3797.

Lopez-Soriano, J., Argiles, J.M., and Lopez-Soriano, F.J. (1996). Lipid metabolism in rats bearing the Yoshida AH-130 ascites hepatoma. Mol. Cell. Biochem. *165*, 17–23.

Mercurio, F., Murray, B.W., Shevchenko, A., Bennett, B.L., Young, D.B., Li, J.W., Pascual, G., Motiwala, A., Zhu, H., Mann, M., and Manning, A.M. (1999). IκB kinase (IKK)-associated protein *1*, a common component of the heterogeneous IKK complex. Mol. Cell. Biol. *19*, 1526–1538.

Moldawer, L.L., Svaninger, G., Gelin, J., and Lundholm, K.G. (1987). Interleukin 1 and tumor necrosis factor do not regulate protein balance in skeletal muscle. Am. J. Physiol. *253*, C766–C773.

Mora, M. (1989). Fibrous-adipose replacement in skeletal muscle biopsy. Eur. Heart J. Suppl. D *10*, 103–104.

Mullen, B.J., Harris, R.B., Patton, J.S., and Martin, R.J. (1990). Recombinant TNF-α chronically administered in rats: lack of cachectic effect. Proc. Soc. Exp. Biol. Med. *193*, 318–325.

Penner, C.G., Gang, G., Wray, C., Fischer, J.E., and Hasselgren, P.O. (2001). The transcription factors NF-κB and AP-1 are differentially regulated in skeletal muscle during sepsis. Biochem. Biophys. Res. Commun. *281*, 1331–1336.

Rossi, F.F., Cangiano, C., Muscaritoli, M., Conversano, L., Torelli, G.F., and Cascino, A. (1995). Tumor-induced changes in host metabolism: a possible marker of neoplastic disease. Nutrition *11*, 595–600.

Rothwarf, D.M., and Karin, M. (2000). The NF-κB activation pathway: a paradigm in information transfer from membrane to nucleus. Science's STKE www.stke.org/cgi/content/full/OC_sigtrans;1999/5/re1.

Sandri, M., Sandri, C., Gilbert, A., Skurk, C., Calabria, E., Picard, A., Walsh, K., Schiaffino, S., Lecker, S.H., and Goldberg, A.L. (2004). Foxo transcription factors induce the atrophy-related ubiquitin ligase atrogin-1 and cause skeletal muscle atrophy. Cell *117*, 399–412.

Stewart, C.E., Newcomb, P.V., and Holly, J.M. (2004). Multifaceted roles of TNF-α in myoblast destruction: a multitude of signal transduction pathways. J. Cell. Physiol. *198*, 237–247.

Stitt, T.N., Drujan, D., Clarke, B.A., Panaro, F., Timofeyva, Y., Kline, W.O., Gonzalez, M., Yancopoulos, G.D., and Glass, D.J. (2004). The IGF-1/PI3K/Akt pathway prevents expression of muscle atrophy-induced ubiquitin ligases by inhibiting FOXO transcription factors. Mol. Cell *14*, 395–403.

Sylla, B.S., Hung, S.C., Davidson, D.M., Hatzivassiliou, E., Malinin, N.L., Wallach, D., Gilmore, T.D., Kieff, E., and Mosialos, G. (1998). Epstein-Barr virus-transforming protein latent infection membrane protein 1 activates transcription factor NF-kappaB through a pathway that includes the NF-κB-inducing kinase and the IκB kinases IKKα and IKKβ. Proc. Natl. Acad. Sci. USA *95*, 10106–10111.

Tawa, N.E., Jr., Odessey, R., and Goldberg, A.L. (1997). Inhibitors of the proteasome reduce the accelerated proteolysis in atrophying rat skeletal muscles. J. Clin. Invest. *100*, 197–203.

Tiao, G., Lieberman, M., Fischer, J.E., and Hasselgren, P.O. (1997). Intracellular regulation of protein degradation during sepsis is different in fast- and slow-twitch muscle. Am. J. Physiol. *272*, R849–R856.

Tisdale, M.J. (1997). Biology of cachexia. J. Natl. Cancer Inst. *89*, 1763–1773.

Van Antwerp, D.J., Martin, S.J., Kafri, T., Green, D.R., and Verma, I.M. (1996). Suppression of TNF-α-induced apoptosis by NF-κB. Science *274*, 787–789.

Wray, C.J., Mammen, J.M., Hershko, D.D., and Hasselgren, P.O. (2003). Sepsis upregulates the gene expression of multiple ubiquitin ligases in skeletal muscle. Int. J. Biochem. Cell Biol. *35*, 698–705.

Yaron, A., Hatzubai, A., Davis, M., Lavon, I., Amit, S., Manning, A.M., Andersen, J.S., Mann, M., Mercurio, F., and Ben Neriah, Y. (1998). Identification of the receptor component of the IκBα-ubiquitin ligase. Nature *396*, 590–594.

Yin, M.J., Yamamoto, Y., and Gaynor, R.B. (1998). The anti-inflammatory agents aspirin and salicylate inhibit the activity of IκB kinase-β. Nature *396*, 77–80.

Yuan, M., Konstantopoulos, N., Lee, J., Hansen, L., Li, Z.W., Karin, M., and Shoelson, S.E. (2001). Reversal of obesity- and diet-induced insulin resistance with salicylates or targeted disruption of *Ikk*b. Science *293*, 1673–1677.